Pulsation of $1\omega_0$ and $2\omega_0$ emission from laser-produced plasmas. I. Experiment

R. A. M. Maddever, B. Luther-Davies, and R. Dragila
Laser Physics Centre, Research School of Physical Sciences, The Australian National University, P.O. Box 4, Canberra, Australian Capital Territory 2601, Australia
(Received 23 January 1989)

We report measurements on time-resolved spectra of the $2\omega_0$ (and, indirectly, $1\omega_0$) emission from plasmas produced by focusing 70–400-psec duration Nd-laser pulses to intensities above $\approx 10^{14}$ W/cm^2 onto planar targets. We observe repeated bursts of the emission lasting only 10–20 psec and typically separated by 30–50 psec. During these bursts the emitted frequency was observed to sweep rapidly across the wavelength band (≈ 50 Å wide), indicating the operation of processes that modulate the emission via phase. The results support our previous work [Dragila, Maddever, and Luther-Davies, Phys. Rev. A **36**, 5292 (1987)], where we concluded that such phase modulation must occur in order to explain the observation that time-integrated spectra obtained in the same conditions were modulated.

I. INTRODUCTION

In recent publications[1,2] we reported measurement of the time-integrated fundamental ($1\omega_0$) and second-harmonic ($2\omega_0$) emission spectra from plasmas produced by focusing the beam from a short-pulse (20–400-psec) Nd-glass laser to high intensity (10^{14}–10^{17} W/cm^2) onto planar solid targets. In these conditions it was concluded that resonance absorption was the main mechanism for second-harmonic generation.[1] These previous experiments were designed to investigate the apparently regular fine structure that modulated the spectra at both frequencies, and which only became clear when very-large-F-number ($F=25$) collection optics were used. The modulation was found to be essentially independent of laser and target parameters and appeared on both $1\omega_0$ and $2\omega_0$ spectra (recent yet unpublished work on $\frac{3}{2}\omega_0$ spectra also revealed modulations) once the laser intensity exceeded about 10^{14} W/cm^2. Furthermore, careful Fourier analysis of the envelope of the spectrum showed that the modulations were, in fact, random. Since background information on time-integrated spectra is essential to this paper,which discusses time resolved spectra, we include in Fig. 1 two samples of time integrated spectra. These correspond to $1\omega_0$ [Fig. 1(a)] and $2\omega_0$ spectra [Fig. 1(b)] recorded at a laser intensity of $\approx 7\times 10^{16}$ and $\approx 10^{16}$ W/cm^2, respectively, from glass targets irradiated at normal incidence by a 70-psec duration 4.0-J Nd-laser pulse. The emission was collected by a lens viewing the target at 45° to the target normal and passed through a 1-m grating monochromator (resolution 0.02 Å) to a Reticon array detector. Note that in these spectra the detector noise is insignificant, as is any structure attributable to imbalance between detector elements within the array, and all the structure corresponds to real spectral modulations. The fact that these modulations were insensitive to parameters of the experiment and appeared on both harmonics led us to search for a relatively simple explanation that could be applied equally to either the $1\omega_0$ or $2\omega_0$

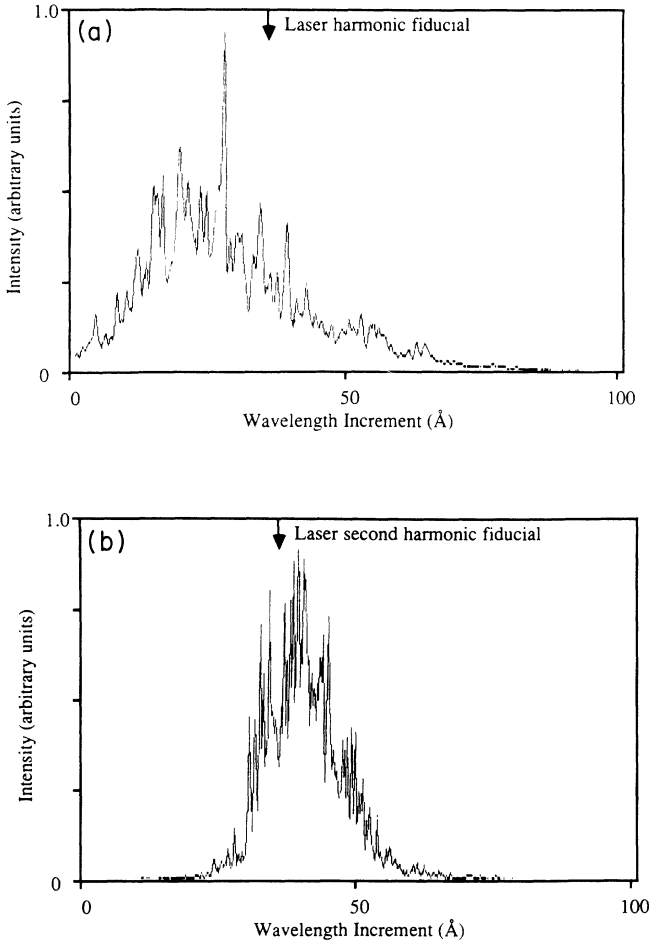

FIG. 1. (a) Example of a time integrated $1\omega_0$ spectrum showing random spectral modulations. Laser intensity was $\approx 7\times 10^{16}$ W/cm^2 and the spectrum was recorded using a Reticon diode array detector at the output of a 1-m spectrograph. (b) A $2\omega_0$ spectrum recorded using the same apparatus for a laser intensity of $\approx 10^{16}$ W/cm^2.

emission. Such an explanation had to be rather insensitive to the physical processes involved in $1\omega_0$ and $2\omega_0$ emission since they are quite different.

Our interpretation of data such as these required an essentially new theory[1] where phase modulation of the emergent waves by the plasma corona generated all the features of the time-integrated spectra (broadening and modulation). All that was required was for the *phase* of the emergent wave to undergo one or several temporal modulations during the laser pulse to cause a rapid frequency sweep of the emission out to one side of the harmonic and back again. The extent of such a sweep defines the extent of the red or blue shift in the time-integrated spectrum while the spectral fine structure has a spacing inversely related to the duration of the phase event. By using a one-dimensional (1D) plasma code we were able to show numerically that the action of the ponderomotive force, which makes the density profile a strong function of laser intensity, was one mechanism that could cause the required phase modulation of the reflected laser light and produce spectra very similar to those observed experimentally. As a consequence of this work it was no longer necessary to invoke a dominant role for the parametric decay instability or stimulated Brillouin scattering to explain the broadening and redshift frequently observed in time-integrated $2\omega_0$ and $1\omega_0$ spectra, respectively.

Since frequency sweeps with a narrow "instantaneous" bandwidth are an inherent feature of the theory involving phase modulation, and fit comfortably with the view that second-harmonic emission, for example, is generated only by resonance absorption, it was of considerable relevance to record time-resolved spectra to search for the predicted frequency sweeping. As a result we are now reporting on an extensive series of experiments where we have characterized the temporal properties of the fundamental and second-harmonic spectra as well as the time dependence of the emission intensity (without spectral resolution). This work supports our previous conclusions from the time-integrated measurements and we have unequivocally observed frequency sweeping of the emission, although the temporal structure is much more complex than the simplest situation consistent with the theory presented in Ref. 1. Specifically, we find that time-resolved spectra are characterized by a series of rapid bursts of emission sweeping rapidly across a wide frequency range with each sweep lasting only 10–20 psec. In some instances these frequency sweeps are accompanied by intensity modulation although, in general, intensity modulations seem to be of secondary importance and accompany the dominant frequency pulsations.

It is the purpose of this paper to describe in detail the experimental work while possible mechanisms leading to the frequency sweeping the pulsations are dealt with in a following publication. Our explanation can, however, be summarized here. We deduce that the plasma contains two "reflecting" surfaces, one located at the critical density, the other is the underdense region of the plasma. The latter reflecting surface can result from a strong density discontinuity such as might exist near quarter critical due to local profile modification associated with the two-plasmon decay instability, or, in our more favored explanation, represents a region with $n \ll n_c$ (n is the local plasma density and n_c the critical density) where stimulated Brillouin scattering (SBS) occurs possibly seeded by the reflection from critical (support for the existence of SBS may be found in Fig. 3 of Ref. 8, which shows that as much as 30% of the incident light, equivalent to about half that *not* absorbed by the plasma, can be either backscattered or reflected through the focusing lens). In both cases it can be shown that as the plasma develops, the reflectivity in the low-density region pulsates, in the former case due to étalon effects and in the latter due to nonliner dephasing processes. A detailed discussion of this behavior is outside the scope of this paper, however, the net effect of these mechanisms is that the reflection point in the plasma moves in time cyclically from near the critical surface to the low-density corona and back. Motion of the reflection point leads to the observed phase modulation and frequency sweeping of reflected light. In the case of $2\omega_0$ emission the critical surface is pumped violently by the reflectivity pulsations leading to cyclic profile modification and phase modulation of the second-harmonic emission.

II. EXPERIMENTAL RESULTS

The experiments were quite straightforward (see Fig. 2) and involved the use of an S-20 Imacom 500 streak camera to resolve via time the intensity of harmonic emission with or without spectral resolution from plasmas produced by focusing horizontally polarized pulses of 1.053-μm Nd-laser radiation onto planar targets made of either glass or lead. The laser pulse duration was in the range 150–400 psec, and the beam was focused onto the targets using an $F=1$ aspheric lens. The focal spot distribution was recorded by reimaging it onto ir-sensitive film, and was then digitized and analyzed by computer to allow the laser intensity to be accurately determined. The target surface was then moved relative to the position of best focus to vary the on-target laser intensity from $\approx 10^{14}-10^{17}$ W/cm^2. A convention was adopted that designate target positions behind the focal plane as nega-

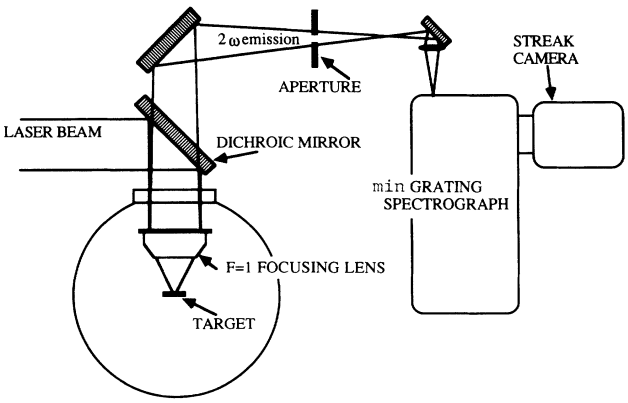

FIG. 2. Experimental apparatus used to record time-resolved $1\omega_0$ and $2\omega_0$ spectra.

tive defocus distances and positions in front of the focal plane as positive defocus distances.

The fact that only a S-20 photocathode was available prevented direct recording of emission at the laser frequency. To overcome this difficulty to some extent, we used a type-II potassium dihydrogen phosphate (KDP) frequency-doubling crystal to convert some of the backscattered 1-μm laser radiation into the visible. Using the refractive index data for KDP,[3] we checked that this crystal had a full width at half maximum (FWHM) bandwidth for second-harmonic generation of 200 Å—about twice the maximum bandwidth recorded in the time-integrated experiments.[1] We concluded, therefore, that the frequency-doubling crystal would not, for reasons of limited bandwidth, distort the spectrum of the 1-μm radiation apart from the inevitable square law dependence of the conversion efficiency with intensity. Nevertheless, most of the time-resolved data were recorded from second-harmonic emission, with checks for consistency with the frequency-doubled 1-μm light being made for completion.

For comparison with the previous time-integrated data the radiation fed to the streak camera was collected using large-F-number optics ($F=20-150$). The actual F number varied depending on the particular experiment and was limited either by the aperture of the collection lends or by slits on the streak camera or spectrograph. When radiation was passed to the streak camera through the spectrograph care was taken to optimize the experimental geometry to ensure the best combination of temporal and spectral resolution was obtained. In these experiments, a trade off exists between good spectral and temporal resolution determined by the uncertainty principle. For a grating of width W and N lines per mm, used in mth order at a wavelength λ, the spectral resolution $\Delta\lambda$ and temporal resolution $\Delta\tau$ are given by

$$\Delta\lambda=\frac{\lambda}{NWm}, \quad \Delta\tau=\frac{NWm\lambda}{c} . \tag{1}$$

Using a 1200-line/mm grating and 9-mm grating width the best temporal resolution was 22 psec (after allowance for the streak camera resolution) while by reducing the grating width to 3 mm, this was improved to <10 psec. The corresponding wavelength resolution was limited by the slit width on the spectrograph to about 1 Å. In the initial experiments a wavelength fiducial was provided by splitting off a portion of the main laser pulse, frequency doubling it, and passing it simultaneously through the spectrograph onto the streak camera. In addition, time-integrated spectra were recorded simultaneously by splitting part of the output of the spectrograph direct to a photographic plate. The limited resolution of the spectrograph, however, prevented the fine spectral modulations such as those in Fig. 1 from being resolved. These initial tests were used to ensure that the basic characteristics of the time-resolved spectra coincided with those of the time-integrated spectra described previously.[1,2] In later experiments, with the best temporal resolution, it proved difficult to incorporate the wavelength fiducial and it was removed.

As mentioned earlier, streak records were also obtained without spectral resolution. In this case the streak camera simply viewed the second-harmonic emission collimated by a lens. Such an experiment is almost trivially easy to set up and immediately reveals amplitude modulations in the recorded signals. A sample result obtained in this manner is shown in Fig. 3. Strong temporal modulations in the emission intensity are quite apparent lasting less than 10 psec and spaced irregularly by 20–50 psec. These data are included since we have found that it can be misleading and include "false" amplitude pulsations depending critically on the exact experimental geometry. The reason for this is related to the presence of a speckle pattern in the recording plane.

Speckle is a well-known phenomenon that arises when coherent light is scattered off or emitted from a rough surface. To our knowledge it has never been discussed in relation to emission from laser-produced plasmas. However, in conditions where the light emitted from the plasma remains partially coherent, it can have some important consequences. Of course for speckle patterns to appear we must assume that the plasma is "rough" on the scale of the wavelength of the laser light. In fact, it would be surprising if in most experiments the plasma was smooth since laser beam nonuniformities, target nonuniformities, various plasma instabilities, and turbulence can all lead to "roughness." In fact, roughness has already been invoked in a number of papers as necessary to explain various experimental observations. For example, Ripin[4] in 1977 reported measurements on the angular distribution of $1\omega_0$ light backscattered from Nd laser produced plasmas at high intensity ($10^{15}-10^{16}$ W/cm^2) and found that the angular spread was essential-

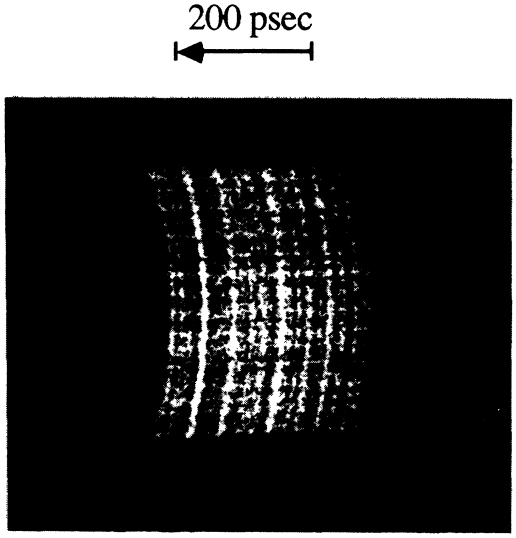

FIG. 3. Streak camera record of backscattered $2\omega_0$ emission recorded without spectral resolution from a Pb target irradiated by a 400-psec Nd-laser pulse of intensity 6×10^{14} W/cm^2. The emission was focused onto a scattering screen located ≈0.5 m in front of the streak camera.

ly independent of the F number of the focusing lens (between $F=1.9$ and 14). In his explanation it was suggested that either strong side scattering was occurring or the plasma was very rough. Similar conclusions arose in the work of Manes *et al.*[5] and Thompson *et al.*[6] where diffuse scattering, corresponding to a 6°–11° rms critical surface roughness, had to be invoked to explain scattering and absorption data, respectively, for Nd-laser produced plasmas. More recently, work in our own laboratory on the angular distribution of second-harmonic emission[7] and absorption[8] both support the idea that the plasma is rough or turbulent in the region near critical. In other words, on the available evidence, speckle patterns could be expected.

The lateral structure in a laser speckle pattern is strictly defined in terms of its autocorrelation function. However, a formula obtained from statistically averaging the distance between adjacent regions of maximum and minimum brightness[9] gives an approximate size σ of the speckles as

$$\sigma \approx 1.2\frac{\lambda z}{D} , \tag{2}$$

where z is the distance of the scattering surface from the observation plane, and D is the diameter of the emitting region. From purely geometrical considerations it can be seen that if a lens of diameter d_1 is used to collect the scattered light then, in a plane some distance from the lens where the output beam has a diameter d_2, the speckle size becomes

$$\sigma' = \sigma\frac{d_2}{d_1} , \tag{3}$$

where σ is the speckle size at the lens itself. In the limit where d_2 corresponds to the image plane of the lens, we have

$$\sigma' = 0.6\lambda/N_a , \tag{4}$$

where N_a is the numerical aperture of the lens. Note that in these conditions the speckle pattern will, in general, be very small and will not affect measurements taken in the image plane.

If the wavelength of the radiation is changed from λ to $\lambda+\Delta\lambda$, then the position of an individual speckle moves angularly at a rate given by

$$\frac{\Delta\phi}{\tan(\phi)} = \frac{\Delta\lambda}{\lambda} , \tag{5}$$

which results in the pattern scanning around as the wavelength of the emission changes. Here ϕ is the angle between the target normal and the observation direction. Our time-integrated spectra[1] would be consistent with a wavelength change $\Delta\lambda$ during the laser pulse such that $\Delta\lambda/\lambda \approx 1/100$. In a situation where, for example, the streak camera viewed the plasma directly (without imaging) at a distance of 30 cm with $\phi=45°$ and the laser spot size was $\approx 60\ \mu$m, then the speckle size would be ≈ 3 mm and the wavelength variation would cause a movement equal to one speckle width across the camera slit. This would result in a false amplitude pulsation being recorded by the camera. Additionally, surface changes during the laser pulse also cause the speckle pattern to move. It is of considerable importance to make sure that the speckle size at the streak camera slit is small in comparison with the slit width—a situation that is not always easy to guarantee as is evident from Eqs. (2) and (3).

Prima facie evidence of speckle patterns produced by laser-produced plasmas was obtained some years ago in experiments in our laboratory where we photographed (without imaging) the $2\omega_0$ beam generated back through the focusing lens in experiments where cylindrical targets between 8 and $\approx 100\ \mu$m in diameter were irradiated with 15–20-psec duration Nd-laser pulses at about 10^{15} W/cm^2. A sample image is shown in Fig. 4 where the granular structure has all the features of a speckle pattern and, for example, the speckle size was found to be inversely proportional to the diameter of the emitting region [in accordance with (2)]. Using longer laser pulses this speckle pattern disappeared probably because it was smeared out.

To search for further evidence of the problem of speckle we designed a simple experiment illustrated in Fig. 5 where the streak camera viewed the emission from the plasma either from a scattering screen or via an optical fiber. The laser spot diameter and geometry of the apparatus was chosen to make the speckle size about equal to the fiber diameter (0.6 mm). Any motion of the speckle pattern would appear in the light transmitted through the fiber, but the larger beam diameter at the screen

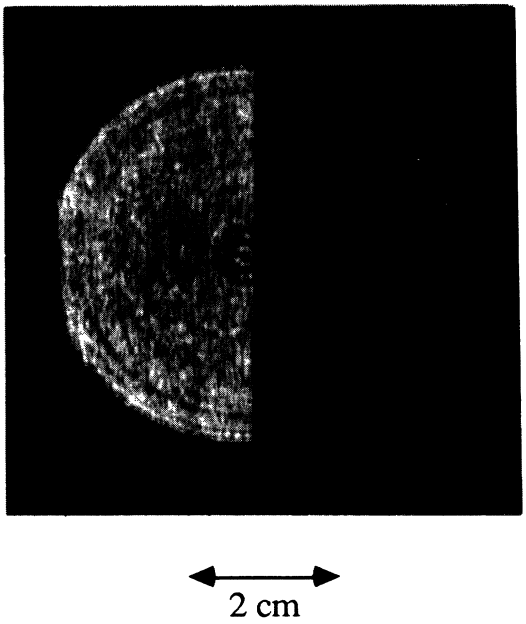

FIG. 4. Speckle pattern recorded by photographing the $2\omega_0$ emission (without imaging) emitted back through the $F=1$ focusing lens. The laser pulse duration was <20 psec and an intensity $\approx 10^{15}$ W/cm^2 was incident on 100-μm-diam glass fiber targets. A neutral density filter was placed over half of the image for film calibration.

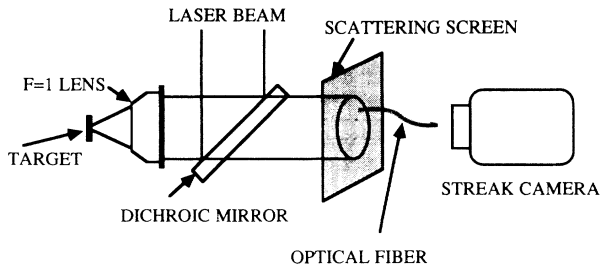

FIG. 5. Experimental arrangement used to investigate the presence of "false" amplitude plusations due to speckle in non-spectrally resolved $2\omega_0$ streaks.

would mean that radiation reaching the slit from that source would, by averaging, not include the effects of speckle. Either $2\omega_0$ emission or frequency-doubled $1\omega_0$ emission were recorded. The geometry of the scattering screen was chosen carefully to ensure that the temporal smearing due to variation in the distance between different points on the screen and the streak camera did not exceed 5 psec. Sample data are shown in Fig. 6. Note that particularly in the case of the frequency-doubled $1\omega_0$ emission, the densitometer scans are much smoother for the radiation from the scattering screen in comparison with that emerging from the fiber. Even for the $2\omega_0$ emission the radiation passing through the fiber shows stronger pulsations. Since ϕ was only $\approx 15°$ in this experiment, any motion of the speckle pattern in response to frequency sweeping of the emission would be limited.

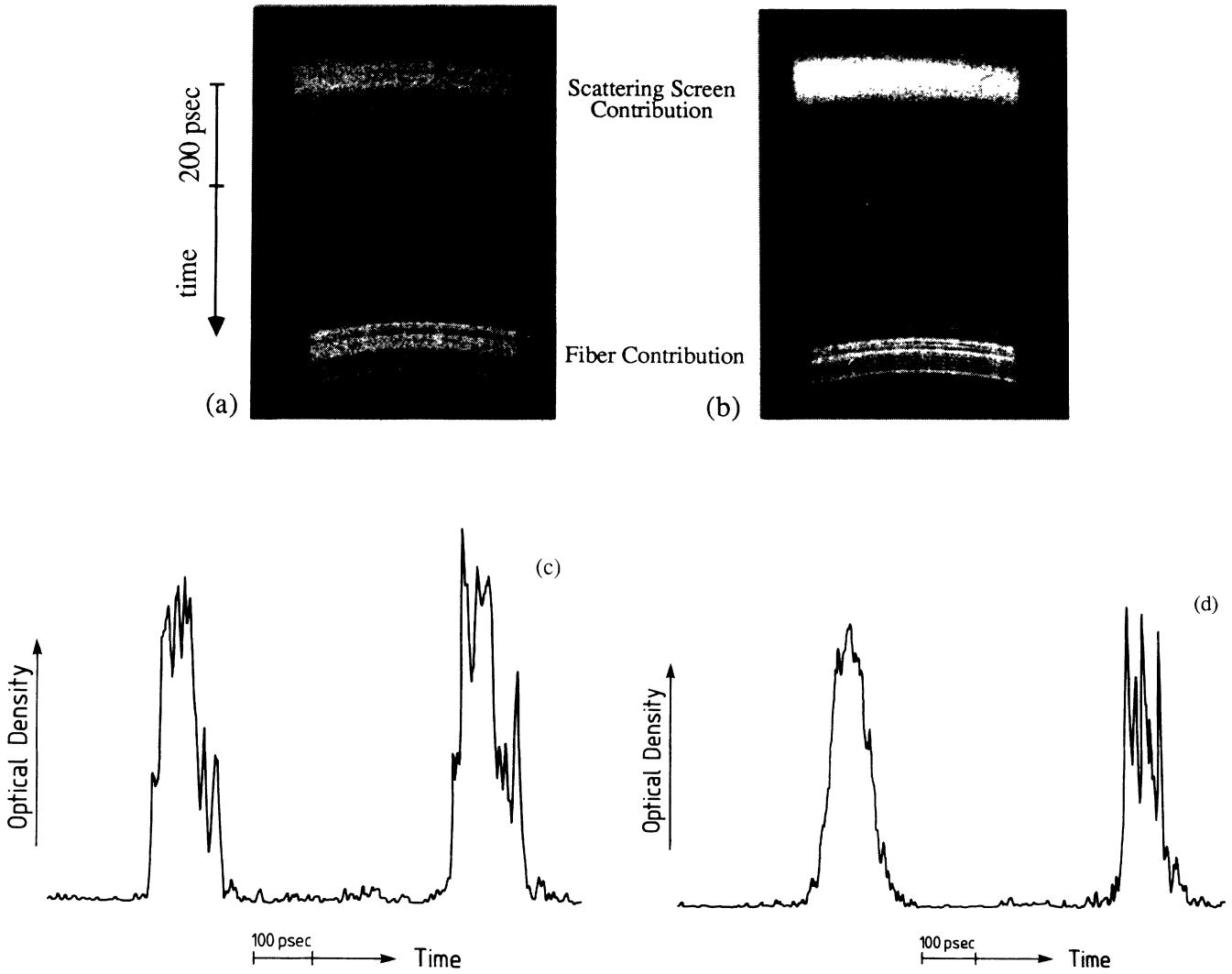

FIG. 6. Streak records obtained from the apparatus shown in Fig. 5. The upper part of the streak records corresponds to the signal from the scattering screen while the lower part comes from the optical fiber. (a) $2\omega_0$ emission using 120-psec duration laser pulse at 3.2×10^{15} W/cm^2; (b) $1\omega_0$ signal viewed after frequency doubling using a KDP crystal. The laser pulse duration was 120 psec and the intensity 6.2×10^{14} W/cm^2. Targets in both cases were glass. (c) and (d) are densitometer scans taken through the center of the data shown in (a) and (b), respectively.

Nevertheless, these data clearly suggest that speckle may at least confuse data from experiments where the emission is time resolved. For example, if the output of a spectrograph were streaked in a condition where motion of a speckle pattern could affect the output signal, a constant amplitude signal sweeping smoothly in frequency would be recorded as a series of pulses in different regions of the spectrum. Obviously the streak records would be misleading.

It should also be noted that speckle patterns would not be produced if the plasma emission occurred simultaneously over a wide bandwidth. The observation of a moving speckle pattern is itself, therefore, a useful diagnostic which places upper bounds on the bandwidth of the particular emission producing the speckle pattern as well as indicating that the emitting plasma has roughness.

With the problem of speckle in mind, care was taken to ensure that subsequent experiments would not be sensitive to it. Scattering screens were positioned appropriately in front of the spectrograph to ensure some averaging of the radiation patterns would occur at the slit. Furthermore, in other experiments the radiation was imaged onto the slit to remove the effect of speckle.

Second-harmonic emission spectra were recorded on the streak camera and sample data are shown in Fig. 7. The four pictures were collected for different negative focusing conditions corresponding to intensities between about 2×10^{14} and 3×10^{15} W/cm^2. For a similar intensity range but positive defoci, results such as those in Fig. 8 were recorded. Note that bursts in time spanning a wide frequency range are apparent in all these data, although the clearest records were obtained in negative defocus positions. This arose because for negative defoci the emission was more evenly spread over the frequency band while for positive defoci it was clumped nearer to the $2\omega_0$ mark.

It is very important to note that the data in Figs. 7 and 8 are not corrected for pincushion distortion in the intensifier optics on the streak camera and hence there is some inherent curvature in the spectra. The nature of

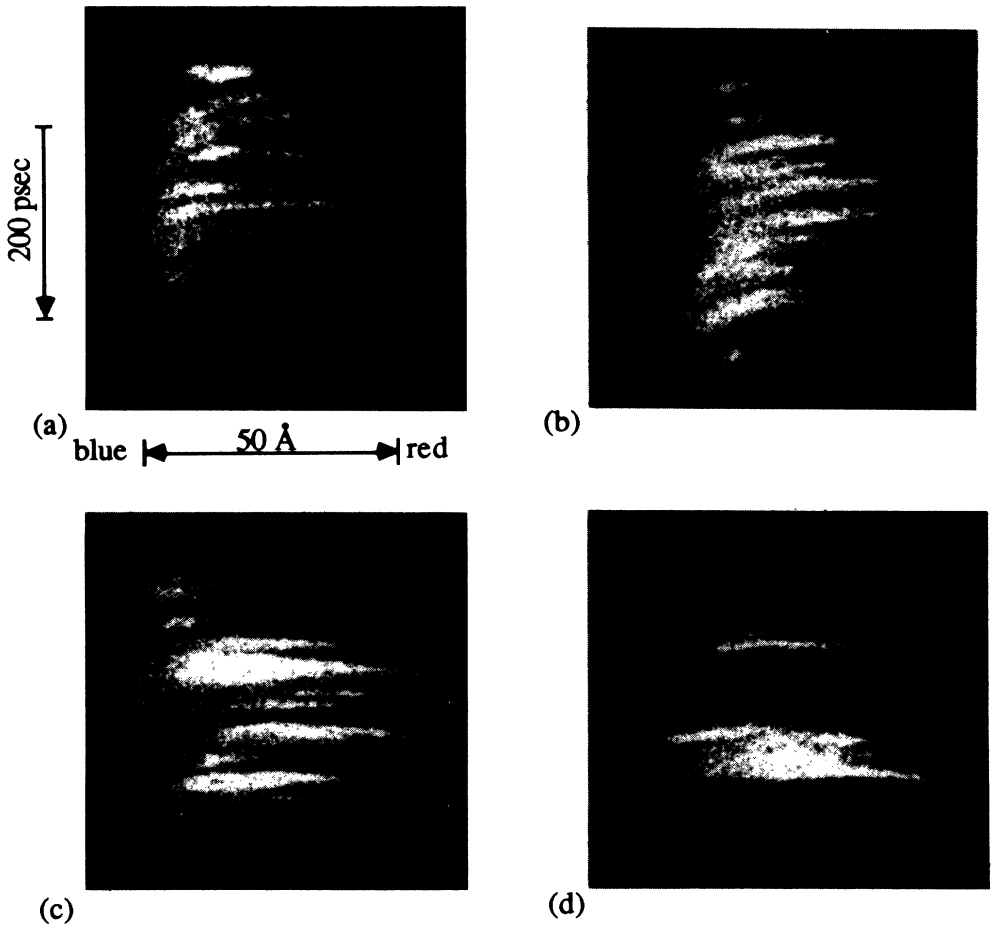

FIG. 7. Streaked $2\omega_0$ spectra recorded from glass targets in negative defocus positions using 220-psec duration laser pulses. The intensities were (a) 4.3×10^{15} W/cm^2, (b) 9.6×10^{14} W/cm^2, (c) 4.1×10^{14} W/cm^2, (d) 2.3×10^{14} W/cm^2.

this distortion is shown in Fig. 9. Clearly the exact frequency versus time behavior could only be obtained after correction for this distortion. Unfortunately, the nature of the data (the very short duration of the bursts) and use of film in the recording process (making accurate registration of the streaks against a reference plane very difficult) prevented useful corrections being made. Nevertheless, careful inspection of data showed clear evidence of frequency sweeping. Examination of Fig. 7(a), for example, reveals that the bursts are far from parallel. Since this feature cannot be due to distortion in the streak camera, this is clear evidence that the emission at different wavelengths does not occur at the same time, but instead, the emission frequency varies more or less continuously during a particular burst. Clear frequency sweeps are not identifiable in every pulsation, but this is understandable since the duration of the bursts is very close to the temporal resolution of the camera-spectrograph combination. It is only when the frequency sweep is broad enough, that it can be detected. The most favorable conditions are in negative defoci at moderate intensities.

Processing the streak records to highlight the trajectories of the bursts helps to clarify the data. Figure 10 shows the locus of the bursts for the data shown in Fig. 7(b). The fact that the trajectories are clearly not parallel provides unequivocal evidence of frequency sweeping. The duration of each burst was typically 10–20 psec while the spacing averaged 30–50 psec.

There was little difference in the nature of the bursts between the lead and glass targets and neither were they affected significantly by laser intensity or pulse duration, although they became far less apparent for positive defocus position as the intensity fell below about 3×10^{14} W/cm^2. These basic characteristics echo our previous observation that the modulations of the time-integrated

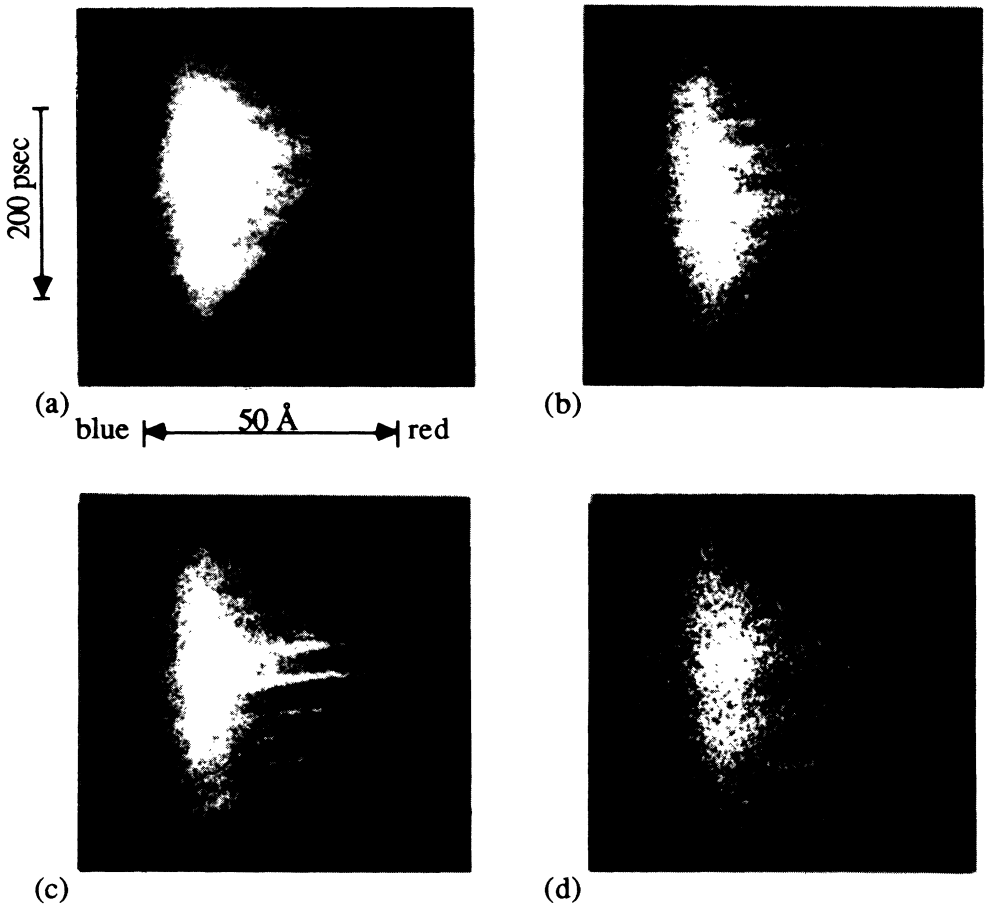

FIG. 8. Streaked $2\omega_0$ spectra recorded from glass targets in positive defocus conditions using 220-psec duration laser pulses. The intensities were (a) $>10^{17}$ W/cm^2, (b) 3.8×10^{15} W/cm^2, (c) 9.2×10^{14} W/cm^2, (d) 4.1×10^{14} W/cm^2.

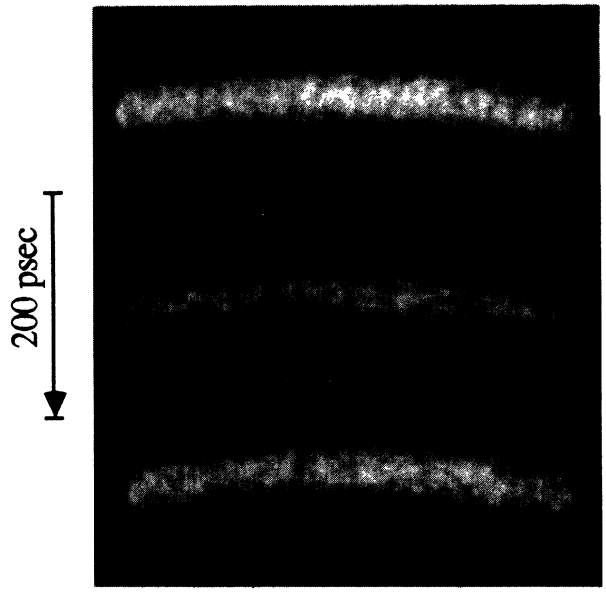

FIG. 9. Pincushion distortion in the streak camera demonstrated by irradiating the camera with a train of 50-psec duration $2\omega_0$ pulses from the laser each separated by 170 psec.

spectra were also insensitive to the same laser and target parameters.[1] Clearly, the insensitivity of both the characteristics of the bursts and the spectral modulations in the time-integrated data to the same parameters provides a firm basis for the belief that they are intimately linked.

Data were also collected by frequency-doubling part of the backreflected $1\omega_0$ light and passing it through the spectrograph to the streak camera. Typical results are shown in Fig. 11. Again bursts were observed and in some cases the spectra were broad enough for frequency sweeping to be evident [Fig. 11(c)]. The bursts had the same basic characteristics as those for the second-harmonic spectra.

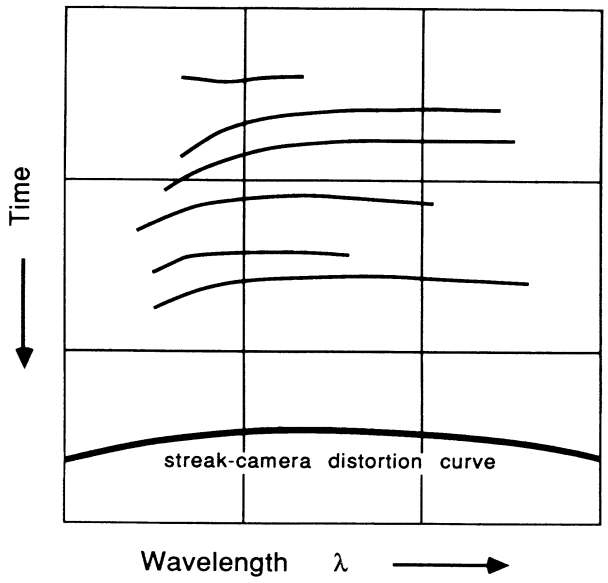

FIG. 10. Data of Fig. 7(b) analyzed to show the trajectories of the main frequency sweeps, together with the characteristic distortion curve of the streak-camera system (from Fig. 9).

III. DISCUSSION

Although only sample data have been presented in this paper, more than a hundred time-resolved spectra have been recorded as part of this study providing us with a wide data base for our conclusions. In addition, we have an even greater body of experimental results on time-integrated spectra, all of which show the irregular fine structure as described in our previous papers.[1,2] Some of the time-resolved spectra show very clear frequency sweeping, although in much of the data the limited temporal resolution and the very short burst duration makes detection of frequency sweeping difficult. On the body of evidence, however, we conclude that frequency sweeping is the *dominant* mechanism determining the spectra and occurs whether we detected it or not. As a result, this implies that the instantaneous emitted bandwidth is relatively narrow, and consistent, for example, with resonance absorption as the main second-harmonic generating process. We can justify our conclusion in part on the basis that frequency sweeping occurs in some of the data (Fig. 10), but it could be argued that other data fail to support this view or are, at best, equivocal and, therefore, we must explain why we can rule out alternative explanations.

The most likely alternative scenario is that the emission occurs simultaneously across a wide spectral band for at least some of the bursts. To test this proposition one has to consider, as we did previously,[1] its result on the time-integrated spectra. Basically, we have shown that time-integrated spectra are broadened, and red (or blue) shifted relative to the laser harmonics. Most importantly, however, they *always* display random spectral modulations. Spectra such as those in Fig. 1 are, however, generated by time-integrating data such as that shown in Figs. 7 and 8. We can, therefore, use this link to argue the case for the dominance of frequency sweeping during bursts even if it was not detectable in the streak records.

There are three major scenarios to be distinguished. First, our favored explanation which supposes that the spectra are formed of bursts, where the frequency sweeps rapidly during each burst and a number of bursts contributes to the total spectrum. This is equivalent to phase and amplitude modulation in time of a carrier frequency. The second scenario is that the emission occurred simultaneously over a wide band in most of the bursts with only a few containing frequency sweeps. The time-integrated spectrum would then be dominated by the contribution obtained by amplitude modulation in time of the broad frequency band. To construct the equivalent time-integrated spectra for these two cases we consider the operations in Fourier space necessary to perform such a construction. In the first case we find ourselves

multiplying the Fourier transform of the frequency spectrum representing the phase event by the Fourier transform of a function representing the amplitude modulation. In the second case we must *convolve* the frequency spectrum representing the broadband emission with the transform of the function representing the amplitude modulation. In the former case the multiplication operation preserves the dominant characteristics of the Fourier transform of the amplitude function (which provides the random spectral modulation), while in the latter case this fine structure disappears since convolution reenforces the characteristics of the broadband structure representing simultaneous emission of a number of frequencies. A third possible scenario is that there are multiple simultaneous frequency peaks that move randomly and pulsate. Such an explanation, however, is inconsistent with the time-integrated spectra since the fine structure contained therein would have to have a bandwidth much larger than is actually observed. Since we have shown that the duration of the bursts of emission is 10 psec, or less, Heisenberg's uncertainty principle tells us immediately that such random bursts of monochromatic light would have a linewidth of 3 Å or more in the $1\omega_0$ time-integrated spectrum and 0.75 Å or more in the $2\omega_0$ spectrum. Even a casual glance shows that these values are broader than the modulations actually observed in the time-integrated data.[1] As a result, it is *only* frequency sweeping accompanied by amplitude modulation that results in the sort of time-integrated spectra we observed experimentally. We regard this as a conclusive argument in favor of our interpretation of these results, which is well supported by the direct observation of frequency sweeping reported here.

The basic characteristics of the bursts of frequency modulated light have been defined from these experiments. Although there is a shot-to-shot variation in the

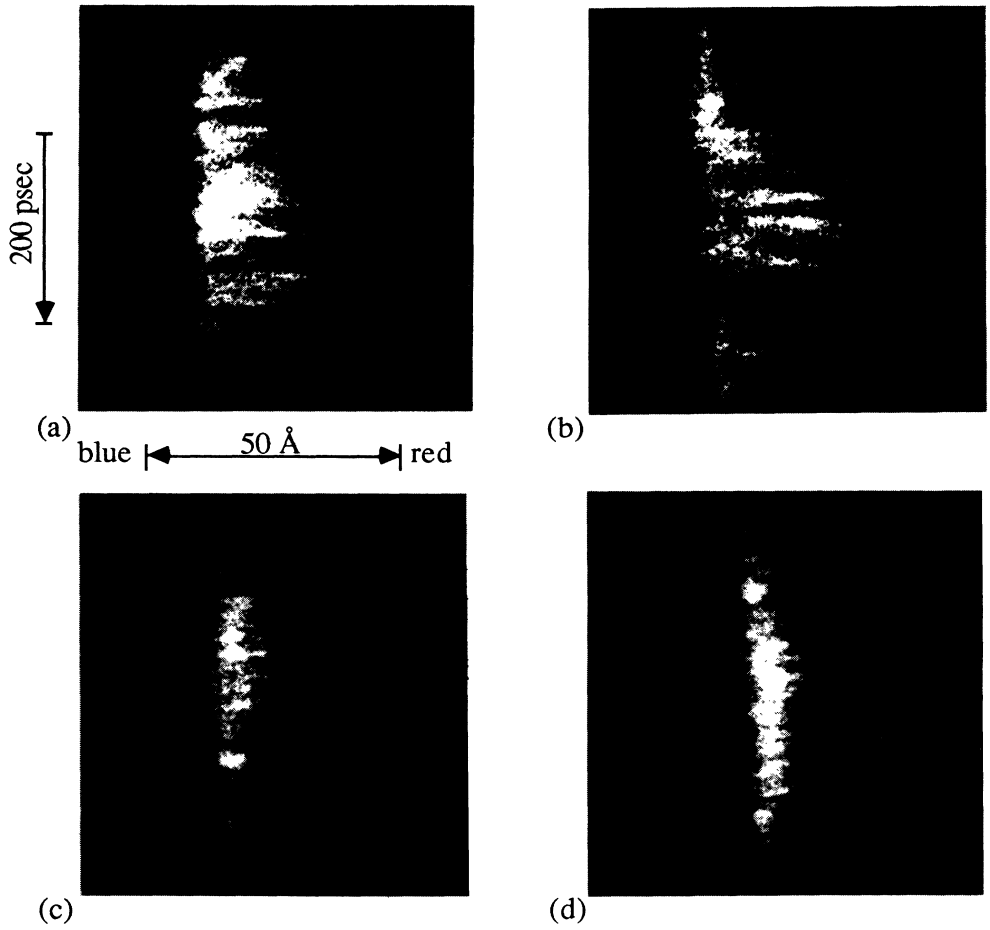

FIG. 11. Examples of streaked $1\omega_0$ spectra (after frequency doubling to enable detection on the $S-20$ streak camera) from glass targets irradiated by 220-psec duration laser pulses. (a) and (b) were for negative defocus positions at 3.8×10^{15} W/cm^2 and 9.8×10^{14} W/cm^2, respectively, while (c) and (d) were for positive defocus positions at 4.0×10^{15} W/cm^2 and 10^{15} W/cm^2, respectively.

characteristics of the spectra even for nominally identical experimental conditions, the average character of the bursts such as their duration and periodicity was remarkably constant over a very wide range of different target and laser parameters. Clearly, these average characteristics were insensitive to pulse duration and laser intensity, for example, although as already noted there appears to be a threshold somewhere near 3×10^{14} W/cm^2 below which the bursts disappear. It is worth noting that this threshold depended to some extent on the irradiation geometry (compare Figs. 7 and 8) since when the target was placed behind the laser focus, the pulsations were considerably stronger than for positive positions. On this point it is important to note that we find distinct changes in the interaction physics between positive and negative defocus positions[8] and the role of such changes would have to be carefully assessed in interpreting these geometry-dependent effects. We consider such details as outside the scope of this paper.

Of more general interest is to compare our results with studies from other laboratories. There is much information in the literature on time-resolved harmonic emission from laser-produced plasmas, both with and without spectral resolution and a sample of that work is given below. In many of the reports, pulsations have been observed (although we are unable to assess the possible role speckle might play in many of these experiments).

In a somewhat different experimental regime from ours was the work of Andreev *et al.*[10] and Gorbunov and Polyanchev[11] where long (5-nsec) Nd-laser pulses irradiated solid targets at moderate intensities ($<5\times10^{14}$ W/cm^2). Streak records of the backscattered fundamental and second-harmonic spectra revealed rather slow temporal modulations on a time scale of 200–700 psec and some spectral modulations (1–2 Å). No satisfactory explanation of these features of the observations were provided although caviton formation was invoked in the work of Andreev. Ripin *et al.*[12] time resolved the spectra of fundamental light from Nd-laser-produced plasmas in conditions similar to ours and observed complex structures in time and wavelength, although no explanation was offered. Tarvin and Schroeder[13] recorded a slow (500-psed) frequency sweep in the light reflected from microballoons illuminated by Nd-laser radiation between 4×10^{14} and 10^{16} W/cm^2, which they attributed to the Doppler shift associated with the implosion of the balloon. However, their data also reveal rapid pulsations in the reflected intensity on the 20-psec time scale, which they apparently attributed to coherence effects in the optics. Grey *et al.*[14] also time resolved the reflected laser light from Nd-laser experiments using 1.6-nsec duration pulses of Nd-laser radiation at 5×10^{15} W/cm^2 and found small-scale temporal and spectral modulations, although this phenomenon was not well understood by the authors.

Time-resolved $2\omega_0$ emission was studied by Jackel, Perry, and Lubin,[15] and pulsations on a 40–60-psec time scale, similar to those reported here, were observed, although no explanation for them was offered. Carter, Sim, and Hughes[16] also studied second-harmonic emission in experiments where 100-psec Nd-laser pulses irradiated glass microballoons at $\approx10^{16}$ W/cm^2 and found intense spectral and temporal modulations—the duration of the bursts being about 10 psec. Results very similar to ours have been reported by Xu, Zhang, and Zhao,[17] using 200-psec Nd-laser pulses incident on planar targets at intensities around 10^{15} W/cm^2. Discrete pulsations separated by 30 psec were observed. Grey *et al.*[14] also studied second-harmonic emission and observed spectrally broad bursts of emission about 15 psec long and separated by 30–40 psec throughout their 1.6-nsec duration laser pulse once the irradiance exceeded $\approx10^{15}$ W/cm^2.

In summary, burst phenomena in $1\omega_0$ and $2\omega_0$ emission have, in fact, been recorded in many laboratories, although none have reported the fast frequency sweeping we observe here. In many cases, however, the temporal resolution of the recording system was not good enough for frequency sweeps to be apparent. Overall, however, fast bursts seem an inherent feature of $1\omega_0$ and $2\omega_0$ emission in a wide range of laser and plasma conditions once the laser intensity exceeds a threshold value in the vicinity of 10^{14} W/cm^2.

As mentioned in the introduction, we do not offer a detailed explanation of the bursts and sweeping behavior here, but are presenting our ideas in a following paper. However, in developing a model to explain these observations, we regard the conclusion that phase modulation and the resulting frequency sweeping are the fundamental processes determining the spectra as absolutely crucial since this highlights the sort of physical processes which must be involved and downgrades the importance of phenomena such as the parametric decay instability (for $2\omega_0$ emission) in the explanation. In brief, we must search for phenomena that can rapidly phase modulate the optical beams. In the case of the reflected radiation a phenomenon causing vary rapid motion of the mirror surface can do this. Clearly this forms the starting point for a satisfactory theory.

[1]R. Dragila, R. A. M. Maddever, and B. Luther-Davies, Phys. Rev. A **36**, 5292 (1987).

[2]M. D. J. Burgess, R. Dragila, and B. Luther-Davies, Opt. Commun. **50**, 236 (1984).

[3]*Handbook of Laser Science and Technology,* edited by M. J. Weber (CRC, Boca Raton, 1986).

[4]B. H. Ripin, Appl. Phys. Lett. **30**, 134 (1977).

[5]K. R. Manes, V. C. Rupert, J. M. Auerbach, P. Lee, and J. E. Swain, Phys. Rev. Lett. **39**, 281 (1977).

[6]J. J. Thomson, W. L. Kruer, A. B. Langdon, C. E. Max, and W. C. Mead, Phys. Fluids **21**, 707 (1978).

[7]G. B. Gillman and B. Luther-Davies, Opt. Commun. **43**, 194 (1982).

[8]A. J. Perry, B. Luther-Davies, and R. Dragila, Phys. Rev. A **39**, 2565 (1989).

[9]A. E. Ennos, in *Laser Speckle and Related Phenomena,* Vol. 9 of *Topics in Applied Physics,* edited by J. C. Dainty (Springer-Verlag, New York, 1975), pp. 203–253.

[10]N. E. Andreev, V. L. Artsimovich, Yu. S. Kas'yanov, V. V. Korobkin, V. P. Silin, and G. L. Stenchikov, Pis'ma Zh.

Eksp. Teor. Fiz. **31**, 639 (1980) [JETP Lett. **31**, 603 (1980)].
[11]L. M. Gorbunov and A. N. Polyanchev, Zh. Eksp. Teor. Fiz. **74**, 552 (1978) [Sov. Phys.—JETP **47**, 290 (1978)].
[12]B. H. Ripin, J. M. McMahon, E. A. McLean, W. M. Manheimer, and J. A. Stemper, Phys. Rev. Lett. **33**, 634 (1974).
[13]J. A. Tarvin and R. J. Schroeder, Phys. Rev. Lett. **47**, 341 (1981).
[14]R. R. Gray, J. Murdoch, S. M. L. Sim, A. J. Cole, R. G. Evans, and W. T. Toner, Plasma Phys. **22**, 967 (1980).
[15]S. Jackel, B. Perry, and M. Lubin, Phys. Rev. Lett. **37**, 95 (1976).
[16]P. D. Carter, S. M. L. Sim, and T. P. Hughes, Opt. Commun. **27**, 423 (1978).
[17]Z. Xu, W. Zhang and S. Zhao, Sci. Sin. **28**, 524 (1985).

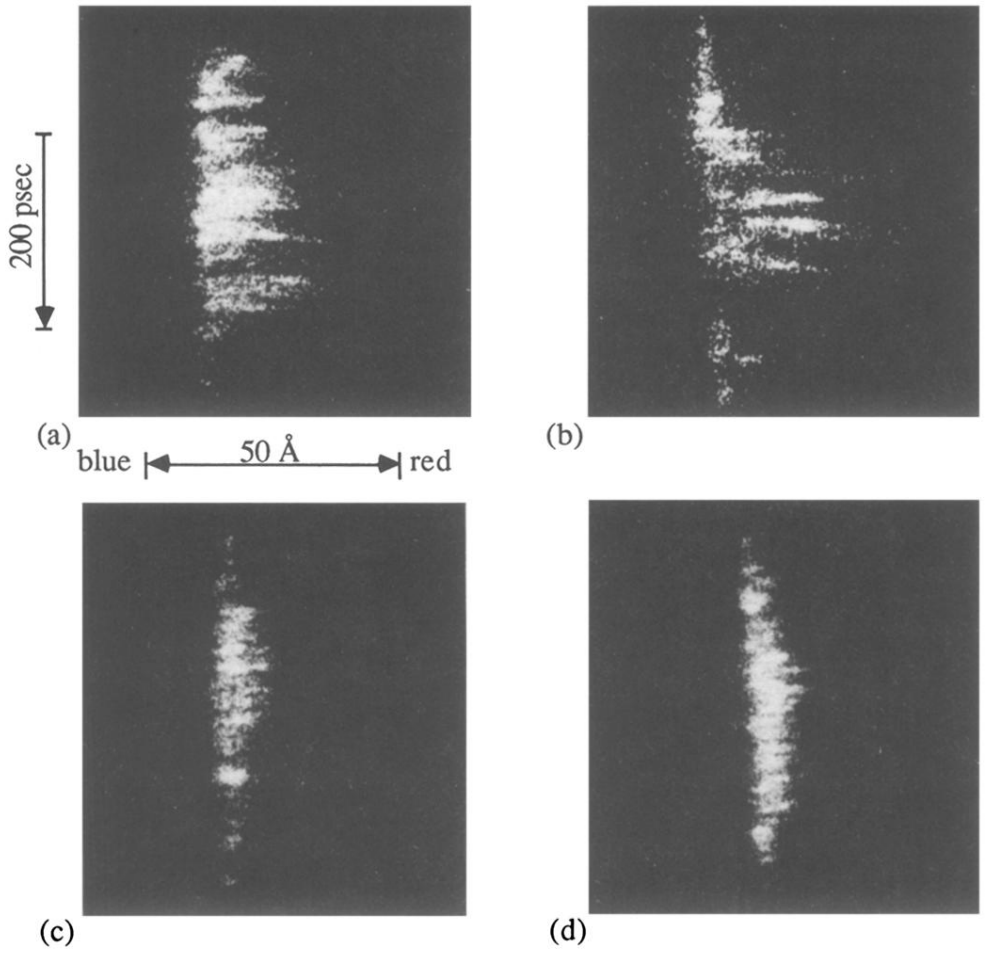

FIG. 11. Examples of streaked $1\omega_0$ spectra (after frequency doubling to enable detection on the $S-20$ streak camera) from glass targets irradiated by 220-psec duration laser pulses. (a) and (b) were for negative defocus positions at 3.8×10^{15} W/cm^2 and 9.8×10^{14} W/cm^2, respectively, while (c) and (d) were for positive defocus positions at 4.0×10^{15} W/cm^2 and 10^{15} W/cm^2, respectively.

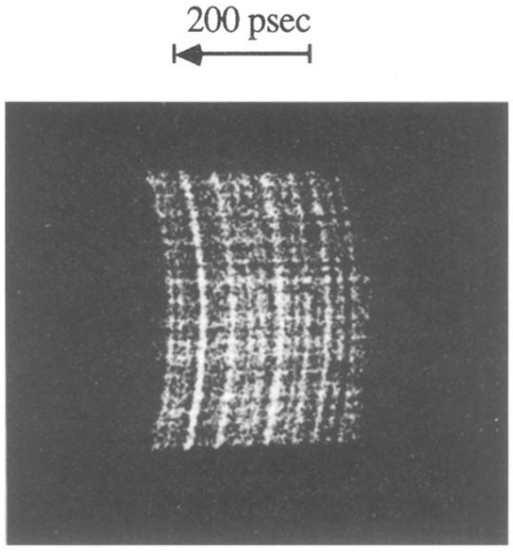

FIG. 3. Streak camera record of backscattered $2\omega_0$ emission recorded without spectral resolution from a Pb target irradiated by a 400-psec Nd-laser pulse of intensity 6×10^{14} W/cm^2. The emission was focused onto a scattering screen located ≈0.5 m in front of the streak camera.

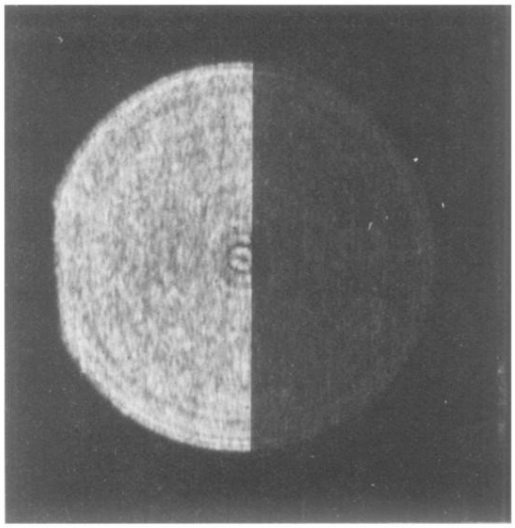

FIG. 4. Speckle pattern recorded by photographing the $2\omega_0$ emission (without imaging) emitted back through the $F=1$ focusing lens. The laser pulse duration was <20 psec and an intensity $\approx 10^{15}$ W/cm^2 was incident on 100-μm-diam glass fiber targets. A neutral density filter was placed over half of the image for film calibration.

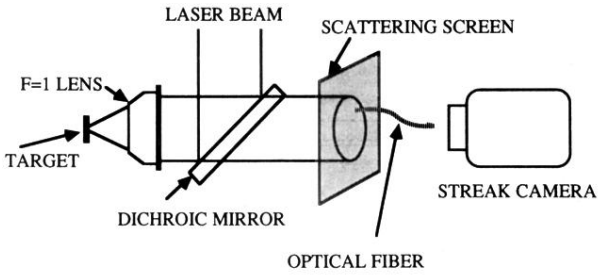

FIG. 5. Experimental arrangement used to investigate the presence of "false" amplitude plusations due to speckle in non-spectrally resolved $2\omega_0$ streaks.

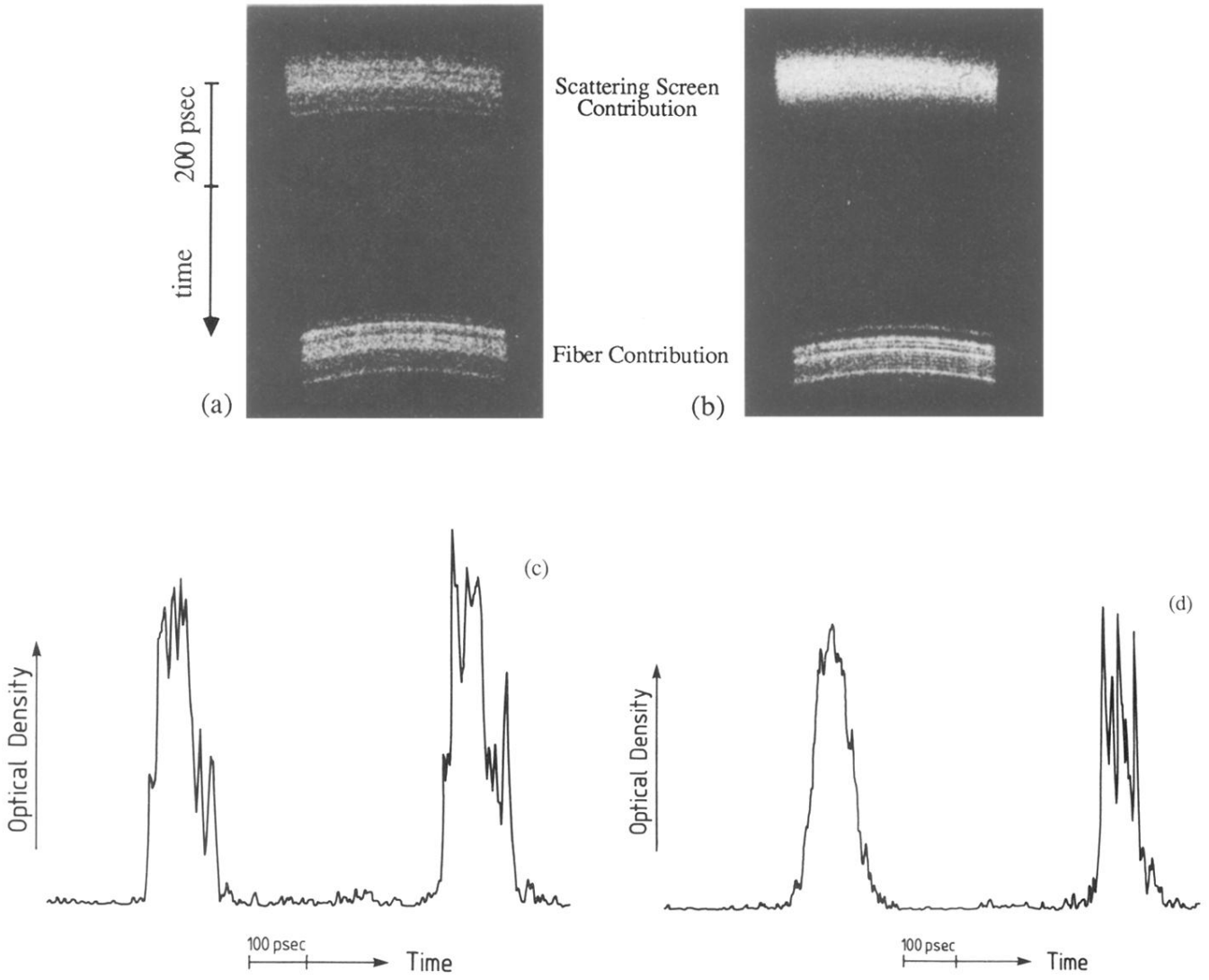

FIG. 6. Streak records obtained from the apparatus shown in Fig. 5. The upper part of the streak records corresponds to the signal from the scattering screen while the lower part comes from the optical fiber. (a) $2\omega_0$ emission using 120-psec duration laser pulse at 3.2×10^{15} W/cm^2; (b) $1\omega_0$ signal viewed after frequency doubling using a KDP crystal. The laser pulse duration was 120 psec and the intensity 6.2×10^{14} W/cm^2. Targets in both cases were glass. (c) and (d) are densitometer scans taken through the center of the data shown in (a) and (b), respectively.

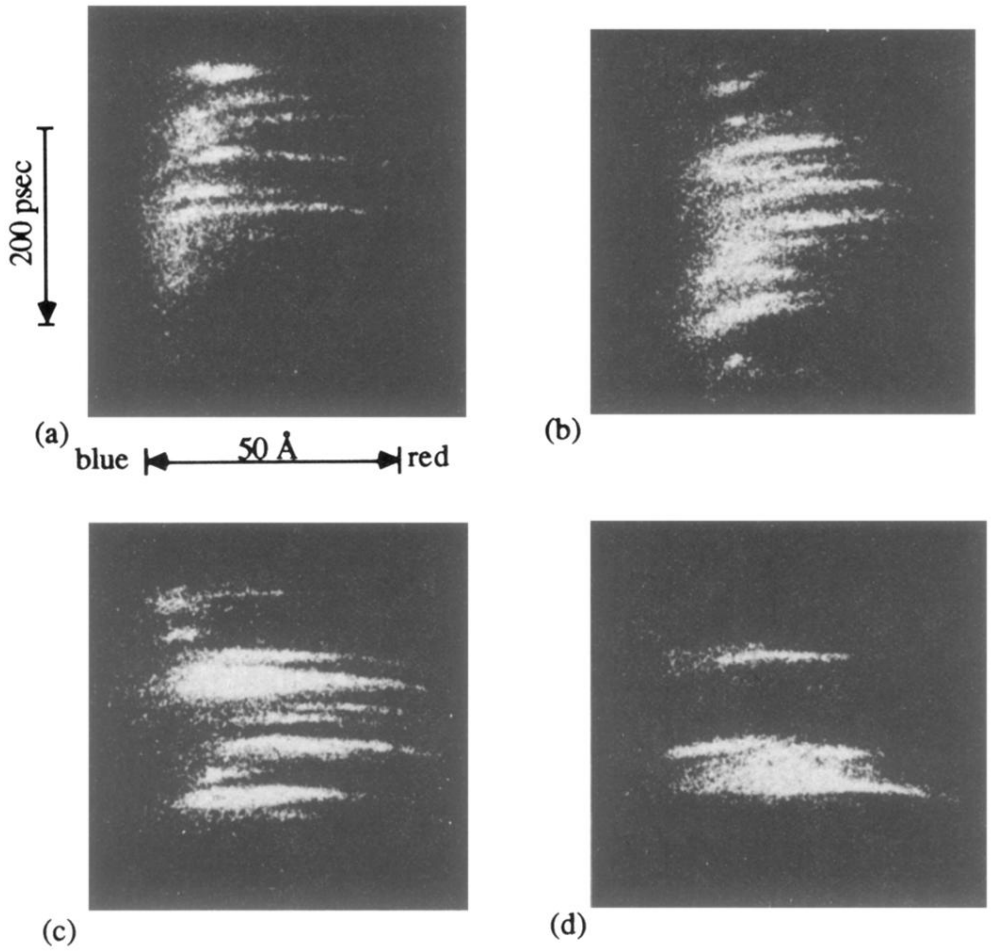

FIG. 7. Streaked $2\omega_0$ spectra recorded from glass targets in negative defocus positions using 220-psec duration laser pulses. The intensities were (a) 4.3×10^{15} W/cm^2, (b) 9.6×10^{14} W/cm^2, (c) 4.1×10^{14} W/cm^2, (d) 2.3×10^{14} W/cm^2.

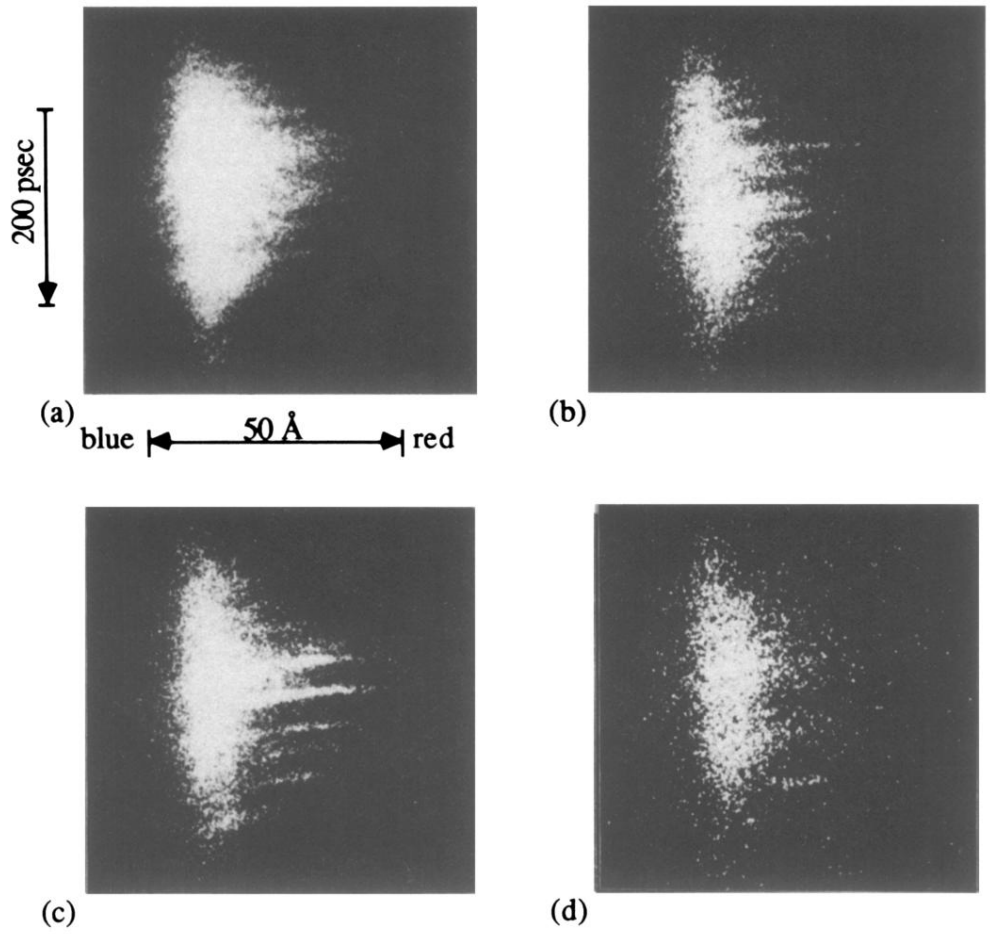

FIG. 8. Streaked $2\omega_0$ spectra recorded from glass targets in positive defocus conditions using 220-psec duration laser pulses. The intensities were (a) $> 10^{17}$ W/cm^2, (b) 3.8×10^{15} W/cm^2, (c) 9.2×10^{14} W/cm^2, (d) 4.1×10^{14} W/cm^2.

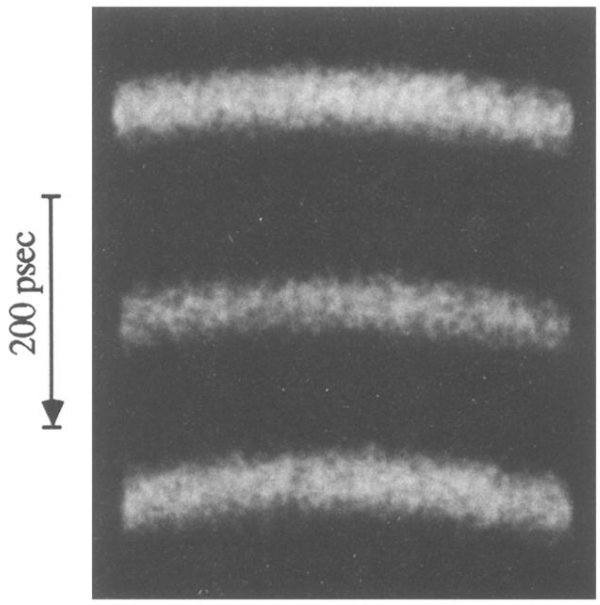

FIG. 9. Pincushion distortion in the streak camera demonstrated by irradiating the camera with a train of 50-psec duration $2\omega_0$ pulses from the laser each separated by 170 psec.